ELSEVIER

International Journal of Solids and Structures 41 (2004) 4407–4422

INTERNATIONAL JOURNAL OF SOLIDS and STRUCTURES

www.elsevier.com/locate/ijsolstr

Two parallel symmetry permeable cracks in functionally graded piezoelectric/piezomagnetic materials under anti-plane shear loading

Zhen-Gong Zhou *, Biao Wang

Center for Composite Materials and Electro-Optics Technology Center, Harbin Institute of Technology, P.O. Box 1247, Harbin 150001, PR China

Received 29 October 2003; received in revised form 1 March 2004
Available online 2 April 2004

Abstract

In this paper, the behavior of two parallel symmetry permeable cracks in functionally graded piezoelectric/piezomagnetic materials subjected to an anti-plane shear loading is investigated. To make the analysis tractable, it is assumed that the material properties c_{44}, e_{15}, ε_{11}, q_{15}, d_{11} and μ_{11} vary exponentially with coordinate parallel to the crack. By using the Fourier transform, the problem can be solved with the help of two pairs of dual integral equations in which the unknown variables are the jumps of the displacements across the crack surfaces. These equations are solved using the Schmidt method. The normalized stress, the electrical displacement and the magnetic flux intensity factors are determined for different geometric for the permeable electric boundary conditions. Numerical examples are provided to show the effect of the geometry of the interacting crack and the parameter β describing the functionally graded materials upon the stress intensity factor of the cracks.

Keywords: Functionally graded piezoelectric/piezomagnetic materials; Schmidt method; Dual integral equations; Parallel cracks

1. Introduction

Combining two or more distinct piezoelectric and piezomagnetic (magnetostrictive) constituents, piezoelectric/piezoemagnetic composite materials is able take the advantages of each constituent and consequently have superior coupling magnetoelectric effect as compared to conventional piezoelectric material or piezomagnetic material. The magnetoelectric coupling is a new product property of the composites, since it is absent in each constituent. In some cases, the coupling effect of piezoelectric/piezomagnetic composites can be even obtained a hundred times larger than that in a single-phase magnetoelectric materials. Consequently, they are extensively used as magnetic field probes, electric packaging, acoustic, hydrophones,

* Corresponding author. Tel.: +86-45186412613; fax: +86-45186418251.
E-mail address: zhouzhg@hit.edu.cn (Z.-G. Zhou).

0020-7683/$ - see front matter © 2004 Elsevier Ltd. All rights reserved.
doi:10.1016/j.ijsolstr.2004.03.004

medical ultrasonic imaging, sensors, and actuators with the responsibility of magneto-electro-mechanical energy conversion (Wu and Huang, 2000). When subjected to mechanical, magnetic and electrical loads in service, these magneto-electro-elastic composites can fail prematurely due to some defects, e.g. cracks, holes, etc. arising during their manufacturing processes. Therefore, it is of great importance to study the magneto-electro-elastic interaction and fracture behaviors of magneto-electro-elastic composites (Sih and Song, 2003; Song and Sih, 2003). The development of piezoelectric/piezomagnetic composites has its roots in the early work of Van Suchtelen (1972) who proposed that the combination of piezoelectric/piezomagnetic phases may exhibit a new material property the magnetoelectric coupling effect. Since then, the magnetoelectric coupling effect of $BaTiO_3$–$CoFe_2O_4$ composites has been measured by many researchers. Much of the theoretical work for the investigation of magnetoelectric coupling effect has only recently been studied in the works (Wu and Huang, 2000; Sih and Song, 2003; Song and Sih, 2003; Harshe et al., 1993; Avellaneda and Harshe, 1994; Nan, 1994; Benveniste, 1995; Huang and Kuo, 1997; Li, 2000). On the other hand, the development of functionally graded materials has demonstrated that they have the potential to reduce the stress concentration and increase of fracture toughness. Consequently, the concept of functionally graded materials can be extended to the piezoelectric/piezomagnetic materials to improve the reliability of piezoelectric/piezomagnetic materials and structures. Some applications of functionally graded piezoelectric materials have been made as discussed in the works of Takagi et al. (2003) and Jin (2003). Recently, Chen et al. (2003), Jin and Zhong (2002), Wang (2003), Soon (2003), Weng and Li (2002) and Li and Weng (2002) analyzed the fracture problems of functionally graded piezoelectric materials. Weng and Li (2002) first considered the static anti-plane problem of a finite crack in functionally graded piezoelectric material strip. Their results showed that the singular stress and electric displacements in functionally graded piezoelectric materials carry the same forms as those in a homogeneous piezoelectric materials but the magnitudes of the intensity factors depend significantly upon the gradient of the functionally graded piezoelectric materials properties. To our knowledge, the electro-magnetic-elastic behavior of functionally graded piezoelectric/piezomagnetic materials with two parallel symmetric permeable cracks subjected to an anti-plane shear loading has not been studied by using the Schmidt method (Morse and Feshbach, 1958; Zhou et al., 1999; Zhou and Wang, 2002).

In this paper, we attempt to extend the concept of functionally graded materials to the piezoelectric/piezomagnetic materials. The magneto-electro-elastic behavior of two parallel symmetric permeable cracks in functionally graded piezoelectric/piezomagnetic materials subjected to an anti-plane shear stress loading is investigated using the Schmidt method (Morse and Feshbach, 1958; Zhou et al., 1999; Zhou and Wang, 2002). Fourier transform is applied and a mixed boundary-value problem is reduced to two pairs of dual integral equations. In solving the dual integral equations, the jumps of the displacements across the crack surfaces are expanded in a series of Jacobi polynomials. This process is quite different from that adopted in previous works (Wu and Huang, 2000; Sih and Song, 2003; Song and Sih, 2003; Van Suchtelen, 1972; Harshe et al., 1993; Avellaneda and Harshe, 1994; Benveniste, 1995; Huang and Kuo, 1997; Li, 2000; Takagi et al., 2003; Jin, 2003; Chen et al., 2003; Jin and Zhong, 2002; Wang, 2003; Soon, 2003; Weng and Li, 2002; Li and Weng, 2002). The form of solution is easy to understand. Numerical solutions are obtained for the stress intensity factors for permeable crack surface conditions.

2. Formulation of the problem

It is assumed that there are two parallel symmetric cracks of length $2l$ in functionally graded piezoelectric/piezomagnetic materials as shown in Fig. 1. h is the distance between two parallel crack. The functionally graded piezoelectric/piezomagnetic materials boundary-value problem for anti-plane shear is considerably simplified if we consider only the out-of-plane displacement, the in-plane electric fields and the in-plane magnetic fields. Since no opening displacement exists for the present anti-plane problem, the crack

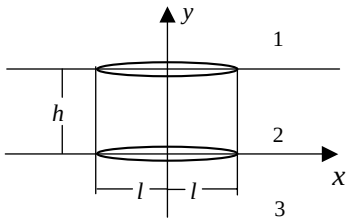

Fig. 1. Two parallel symmetric cracks functionally graded piezoelectric/piezomagnetic materials.

surfaces can be assumed to be in perfect contact. Accordingly, permeable condition will be enforced in the present study, i.e., both the electric potential and the normal electric displacement are assumed to be continuous across the crack surfaces. So the boundary conditions of the present problem are (In this paper, we just consider the perturbation field.)

$$\begin{cases} \tau_{yz}^{(1)}(x,h^+) = \tau_{yz}^{(2)}(x,h^-) = -\tau_0(x), & |x| \leqslant l \\ w^{(1)}(x,h^+) = w^{(2)}(x,h^-), & |x| > l \\ \tau_{yz}^{(2)}(x,0^+) = \tau_{yz}^{(3)}(x,0^-) = -\tau_0(x), & |x| \leqslant l \\ w^{(2)}(x,0^+) = w^{(3)}(x,0^-), & |x| > l \end{cases} \tag{1}$$

$$\begin{cases} \phi^{(1)}(x,h^+) = \phi^{(2)}(x,h^-), & D_y^{(1)}(x,h^+) = D_y^{(2)}(x,h^-) \\ \psi^{(1)}(x,h^+) = \psi^{(2)}(x,h^-), & B_y^{(1)}(x,h^+) = B_y^{(2)}(x,h^-) \\ \phi^{(2)}(x,0^+) = \phi^{(3)}(x,0^-), & D_y^{(2)}(x,0^+) = D_y^{(3)}(x,0^-) \\ \psi^{(2)}(x,0^+) = \psi^{(3)}(x,0^-), & B_y^{(2)}(x,0^+) = B_y^{(3)}(x,0^-) \end{cases}, \qquad |x| < \infty \tag{2}$$

$$w^{(1)}(x,y) = w^{(2)}(x,y) = w^{(3)}(x,y) = 0 \quad \text{for } (x^2+y^2)^{1/2} \to \infty \tag{3}$$

In this paper, $\tau_0(x)$ is the anti-plane shear loading. Also note that all quantities with superscript k ($k = 1, 2, 3$) refer to the upper half plane 1, the layer 2 and the lower half plane 3 as shown in Fig. 1, respectively.

Crack problems in the non-homogeneous piezoelectric/piezomagnetic materials do not appear to be analytically tractable for arbitrary variations of material properties. Usually, one tries to generate the forms of non-homogeneities for which the problem becomes tractable. Similar to the treatment of the crack problem for isotropic non-homogeneous materials in previous works (Delale and Erdogan, 1988; Fildis and Yahsi, 1996; Ozturk and Erdogan, 1997), we assume the material properties are described by:

$$\begin{aligned} &c_{44} = c_{440}\,\mathrm{e}^{\beta x}, \qquad e_{15} = e_{150}\,\mathrm{e}^{\beta x}, \qquad \varepsilon_{11} = \varepsilon_{110}\,\mathrm{e}^{\beta x}, \qquad q_{15} = q_{150}\,\mathrm{e}^{\beta x}, \qquad d_{11} = d_{110}\,\mathrm{e}^{\beta x}, \\ &\mu_{11} = \mu_{110}\,\mathrm{e}^{\beta x} \end{aligned} \tag{4}$$

where c_{440} is shear modulus, e_{150} is piezoelectric coefficient, ε_{110} is dielectric parameter, q_{150} is piezomagnetic coefficient, d_{110} is magnetoelectric coefficient, μ_{110} is magnetic permeability. β is the functionally graded parameter.

The constitutive equations for the mode III crack can be expressed as

$$\tau_{zk}^{(i)} = c_{44} w_{,k}^{(i)} + e_{15}\phi_{,k}^{(i)} + q_{15}\psi_{,k}^{(i)} \quad (k = x, y, \ \ i = 1, 2, 3) \tag{5}$$

$$D_k^{(i)} = e_{15} w_{,k}^{(i)} - \varepsilon_{11}\phi_{,k}^{(i)} - d_{11}\psi_{,k}^{(i)} \quad (k = x, y, \ \ i = 1, 2, 3) \tag{6}$$

$$B_k^{(i)} = q_{15} w_{,k}^{(i)} - d_{11}\phi_{,k}^{(i)} - \mu_{11}\psi_{,k}^{(i)} \quad (k = x, y, \ \ i = 1, 2, 3) \tag{7}$$

The anti-plane governing equations are

$$c_{440}\left(\nabla^2 w^{(k)}+\beta\frac{\partial w^{(k)}}{\partial x}\right)+e_{150}\left(\nabla^2\phi^{(k)}+\beta\frac{\partial\phi^{(k)}}{\partial x}\right)+e_{150}\left(\nabla^2\psi^{(k)}+\beta\frac{\partial\psi^{(k)}}{\partial x}\right)=0 \tag{8}$$

$$e_{150}\left(\nabla^2 w^{(k)}+\beta\frac{\partial w^{(k)}}{\partial x}\right)-\varepsilon_{110}\left(\nabla^2\phi^{(k)}+\beta\frac{\partial\phi^{(k)}}{\partial x}\right)-d_{110}\left(\nabla^2\psi^{(k)}+\beta\frac{\partial\psi^{(k)}}{\partial x}\right)=0 \tag{9}$$

$$q_{150}\left(\nabla^2 w^{(i)}+\beta\frac{\partial w^{(k)}}{\partial x}\right)-d_{110}\left(\nabla^2\phi^{(i)}+\beta\frac{\partial\phi^{(k)}}{\partial x}\right)-\mu_{110}\left(\nabla^2\psi^{(i)}+\beta\frac{\partial\psi^{(k)}}{\partial x}\right)=0 \tag{10}$$

where $\nabla^2=\partial^2/\partial x^2+\partial^2/\partial y^2$ is the two dimensional Laplace operator.

3. Solution

The system of above governing equations is solved using the Fourier integral transform technique. The general expressions for the displacement components, the electric potential and the magnetic potential can be obtained as follows:

$$\begin{cases} w^{(1)}(x,y)=\dfrac{1}{2\pi}\displaystyle\int_{-\infty}^{\infty}A_1(s)\,\mathrm{e}^{-\gamma y}\,\mathrm{e}^{-\mathrm{i}sx}\,\mathrm{d}s \\ \phi^{(1)}(x,y)=a_0 w^{(1)}(x,y)+\dfrac{1}{2\pi}\displaystyle\int_{-\infty}^{\infty}B_1(s)\,\mathrm{e}^{-\gamma y}\,\mathrm{e}^{-\mathrm{i}sx}\,\mathrm{d}s\,, \quad y\geqslant h \\ \psi^{(1)}(x,y)=a_1 w^{(1)}(x,y)+\dfrac{1}{2\pi}\displaystyle\int_{-\infty}^{\infty}C_1(s)\,\mathrm{e}^{-\gamma y}\,\mathrm{e}^{-\mathrm{i}sx}\,\mathrm{d}s \end{cases} \tag{11}$$

$$\begin{cases} w^{(2)}(x,y)=\dfrac{1}{2\pi}\displaystyle\int_{-\infty}^{\infty}[A_2(s)\,\mathrm{e}^{-\gamma y}+B_2(s)\,\mathrm{e}^{\gamma y}]\,\mathrm{e}^{-isx}\,\mathrm{d}s \\ \phi^{(2)}(x,y)=a_0 w^{(2)}(x,y)+\dfrac{1}{2\pi}\displaystyle\int_{-\infty}^{\infty}[C_2(s)\,\mathrm{e}^{-\gamma y}+D_2(s)\,\mathrm{e}^{\gamma y}]\,\mathrm{e}^{-\mathrm{i}sx}\,\mathrm{d}s\,, \quad 0\leqslant y\leqslant h \\ \psi^{(2)}(x,y)=a_1 w^{(2)}(x,y)+\dfrac{1}{2\pi}\displaystyle\int_{-\infty}^{\infty}[E_2(s)\,\mathrm{e}^{-\gamma y}+F_2(s)\,\mathrm{e}^{\gamma y}]\,\mathrm{e}^{-\mathrm{i}sx}\,\mathrm{d}s \end{cases} \tag{12}$$

$$\begin{cases} w^{(3)}(x,y)=\dfrac{1}{2\pi}\displaystyle\int_{-\infty}^{\infty}A_3(s)\,\mathrm{e}^{\gamma y}\,\mathrm{e}^{-\mathrm{i}sx}\,\mathrm{d}s \\ \phi^{(3)}(x,y)=a_0 w^{(3)}(x,y)+\dfrac{1}{2\pi}\displaystyle\int_{-\infty}^{\infty}B_3(s)\,\mathrm{e}^{\gamma y}\,\mathrm{e}^{-\mathrm{i}sx}\,\mathrm{d}s\,, \quad y\leqslant 0 \\ \psi^{(3)}(x,y)=a_1 w^{(3)}(x,y)+\dfrac{1}{2\pi}\displaystyle\int_{0}^{\infty}C_3(s)\,\mathrm{e}^{\gamma y}\,\mathrm{e}^{-\mathrm{i}sx}\,\mathrm{d}s \end{cases} \tag{13}$$

where $A_1(s)$, $B_1(s)$, $C_1(s)$, $A_2(s)$, $B_2(s)$, $C_2(s)$, $D_2(s)$, $E_2(s)$, $F_2(s)$ $A_3(s)$, $B_3(s)$ and $C_3(s)$ are unknown functions, $\gamma=\sqrt{\mathrm{i}\beta+s^2}$, $a_0=\frac{\mu_{11}e_{15}-d_{11}q_{15}}{\varepsilon_{11}\mu_{11}-d_{11}^2}$, $a_1=\frac{q_{15}\varepsilon_{11}-d_{11}e_{15}}{\varepsilon_{11}\mu_{11}-d_{11}^2}$.

So from Eqs. (5)–(7), we have

$$\tau_{yz}^{(1)}(x,y)=-\frac{\mathrm{e}^{\beta x}}{2\pi}\int_{-\infty}^{\infty}\gamma[(c_{440}+a_0e_{150}+a_1q_{150})A_1(s)+e_{150}B_1(s)+q_{150}C_1(s)]\,\mathrm{e}^{-\gamma y}\,\mathrm{e}^{-\mathrm{i}sx}\,\mathrm{d}s \tag{14}$$

$$D_y^{(1)}(x,y) = \frac{e^{\beta x}}{2\pi}\int_{-\infty}^{\infty}\gamma[\varepsilon_{110}B_1(s) + d_{110}C_1(s)]\,e^{-\gamma y}e^{-isx}\,ds \tag{15}$$

$$B_y^{(1)}(x,y) = \frac{e^{\beta x}}{2\pi}\int_{-\infty}^{\infty}\gamma[d_{110}B_1(s) + \mu_{110}C_1(s)]\,e^{-\gamma y}e^{-isx}\,ds \tag{16}$$

$$\begin{aligned}\tau_{yz}^{(2)}(x,y) = -\frac{e^{\beta x}}{2\pi}\int_{-\infty}^{\infty}\gamma\{&[(c_{440} + a_0e_{150} + a_1q_{150})A_2(s) + e_{150}C_2(s) + q_{150}E_2(s)]\,e^{-\gamma y}\\ &- [(c_{440} + a_0e_{150} + a_1q_{150})B_2(s) + e_{150}D_2(s) + q_{150}F_2(s)]\,e^{\gamma y}\}\,e^{-isx}\,ds\end{aligned} \tag{17}$$

$$D_y^{(2)}(x,y) = \frac{e^{\beta x}}{2\pi}\int_{-\infty}^{\infty}\gamma\{[\varepsilon_{110}C_2(s) + d_{110}E_2(s)]\,e^{-\gamma y} - [\varepsilon_{110}D_2(s) + d_{110}F_2(s)]\,e^{\gamma y}\}\,e^{-isx}\,ds \tag{18}$$

$$B_y^{(2)}(x,y) = \frac{e^{\beta x}}{2\pi}\int_{-\infty}^{\infty}\gamma\{[d_{110}C_2(s) + \mu_{110}E_2(s)]\,e^{-\gamma y} - [d_{110}D_2(s) + \mu_{110}F_2(s)]\,e^{\gamma y}\}\,e^{-isx}\,ds \tag{19}$$

$$\tau_{yz}^{(3)}(x,y) = \frac{e^{\beta x}}{2\pi}\int_{-\infty}^{\infty}\gamma[(c_{440} + a_0e_{150} + a_1q_{150})A_3(s) + e_{150}B_3(s) + q_{150}C_3(s)]\,e^{\gamma y}e^{-isx}\,ds \tag{20}$$

$$D_y^{(3)}(x,y) = -\frac{e^{\beta x}}{2\pi}\int_{-\infty}^{\infty}\gamma[\varepsilon_{110}B_3(s) + d_{110}C_3(s)]\,e^{\gamma y}e^{-isx}\,ds \tag{21}$$

$$B_y^{(3)}(x,y) = -\frac{e^{\beta x}}{2\pi}\int_{-\infty}^{\infty}\gamma[d_{110}B_3(s) + \mu_{110}C_3(s)]\,e^{\gamma y}e^{-isx}\,ds \tag{22}$$

To solve the problem, the jumps of the displacements, the electric and the magnetic potentials across the crack surfaces are defined as follows:

$$f_1(x) = w^{(1)}(x,h^+) - w^{(2)}(x,h^-) \tag{23}$$

$$f_2(x) = w^{(2)}(x,0^+) - w^{(3)}(x,0^-) \tag{24}$$

$$f_{\phi 1}(x) = \phi^{(1)}(x,h^+) - \phi^{(2)}(x,h^-) \tag{25}$$

$$f_{\phi 2}(x) = \phi^{(2)}(x,0^+) - \phi^{(3)}(x,0^-) \tag{26}$$

$$f_{\psi 1}(x) = \psi^{(1)}(x,h^+) - \psi^{(2)}(x,h^-) \tag{27}$$

$$f_{\psi 2}(x) = \psi^{(2)}(x,0^+) - \psi^{(3)}(x,0^-) \tag{28}$$

Substituting Eqs. (11)–(13) into Eqs. (23)–(28), and applying the Fourier transform and the boundary conditions, it can be obtained

$$A_1(s)\,e^{-\gamma h} - A_2(s)\,e^{-\gamma h} - B_2(s)\,e^{\gamma h} = \bar{f}_1(s) \tag{29}$$

$$A_2(s) + B_2(s) - A_3(s) = \bar{f}_2(s) \tag{30}$$

$$a_0[A_1(s)\,e^{-\gamma h} - A_2(s)\,e^{-\gamma h} - B_2(s)\,e^{\gamma h}] + B_1(s)\,e^{-\gamma h} - C_2(s)\,e^{-sh} - D_2(s)\,e^{\gamma h} = 0 \tag{31}$$

$$a_0[A_1(s)+B_2(s)-A_3(s)]+C_2(s)+D_2(s)-B_3(s)=0 \tag{32}$$

$$a_1[A_1(s)\,\mathrm{e}^{-\gamma h}-A_2(s)\,\mathrm{e}^{-\gamma h}-B_2(s)\,\mathrm{e}^{\gamma h}]+C_1(s)\,\mathrm{e}^{-\gamma h}-E_2(s)\,\mathrm{e}^{-\gamma h}-F_2(s)\,\mathrm{e}^{\gamma h}=0 \tag{33}$$

$$a_1[A_2(s)+B_2(s)-A_3(s)]+E_2(s)+F_2(s)-C_3(s)=0 \tag{34}$$

A superposed bar indicates the Fourier transform throughout the paper. Substituting Eqs. (14)–(22) into Eqs. (1) and (2), it can be obtained

$$\begin{aligned}&[(c_{440}+a_0e_{150}+a_1q_{150})A_1(s)+e_{150}B_1(s)+q_{150}C_1(s)]\,\mathrm{e}^{-\gamma h}-[(c_{440}+a_0e_{150}+a_1q_{150})A_2(s)+e_{150}C_2(s)\\&\quad+q_{150}E_2(s)]\,\mathrm{e}^{-\gamma h}+[(c_{440}+a_0e_{150}+a_1q_{150})B_2(s)+e_{150}D_2(s)+q_{150}F_2(s)]\,\mathrm{e}^{\gamma h}=0\end{aligned} \tag{35}$$

$$\begin{aligned}&(c_{440}+a_0e_{150}+a_1q_{150})A_2(s)+e_{150}C_2(s)+q_{150}E_2(s)-[(c_{440}+a_0e_{150}+a_1q_{150})B_2(s)+e_{150}D_2(s)\\&\quad+q_{150}F_2(s)]+[(c_{440}+a_0e_{150}+a_1q_{150})A_3(s)+e_{150}B_3(s)+q_{150}C_3(s)]=0\end{aligned} \tag{36}$$

$$-[\varepsilon_{110}B_1(s)+d_{110}C_1(s)]\,\mathrm{e}^{-\gamma h}+[\varepsilon_{110}C_2(s)+d_{110}E_2(s)]\,\mathrm{e}^{-\gamma h}-[\varepsilon_{110}D_2(s)+d_{110}F_2(s)]\,\mathrm{e}^{\gamma h}=0 \tag{37}$$

$$-\varepsilon_{110}C_2(s)-d_{110}E_2(s)+\varepsilon_{110}D_2(s)+d_{110}F_2(s)-\varepsilon_{110}B_3(s)-d_{110}C_3(s)=0 \tag{38}$$

$$[-d_{110}B_1(s)-\mu_{110}C_1(s)]\,\mathrm{e}^{-\gamma h}+[d_{110}C_2(s)+\mu_{110}E_2(s)]\,\mathrm{e}^{-\gamma h}-[d_{110}D_2(s)+\mu_{110}F_2(s)]\,\mathrm{e}^{\gamma h}=0 \tag{39}$$

$$[-d_{110}C_2(s)-\mu_{110}E_2(s)+d_{110}D_2(s)+\mu_{110}F_2(s)]-d_{110}B_3(s)-\mu_{110}C_3(s)=0 \tag{40}$$

By solving 12 Eqs. (29)–(40) with 12 unknown functions $A_1(s)$, $B_1(s)$, $C_1(s)$, $A_2(s)$, $B_2(s)$, $C_2(s)$, $D_2(s)$, $E_2(s)$, $F_2(s)$ $A_3(s)$, $B_3(s)$ and $C_3(s)$ and applying the boundary conditions (1) and (2), it can be obtained:

$$\frac{1}{2\pi}\int_{-\infty}^{\infty}\bar{f}_1(s)\,\mathrm{e}^{-\mathrm{i}sx}\,\mathrm{d}s=0,\quad |x|>l \tag{41}$$

$$\frac{1}{2\pi}\int_{-\infty}^{\infty}\bar{f}_2(s)\,\mathrm{e}^{-\mathrm{i}sx}\,\mathrm{d}s=0,\quad |x|>l \tag{42}$$

$$\frac{c_{440}\,\mathrm{e}^{\beta x}}{4\pi}\int_{-\infty}^{\infty}\gamma[\bar{f}_1(s)+\mathrm{e}^{-\gamma h}\bar{f}_2(s)]\,\mathrm{e}^{-\mathrm{i}sx}\,\mathrm{d}s=\tau_0(x),\quad |x|\leqslant l \tag{43}$$

$$\frac{c_{440}\,\mathrm{e}^{\beta x}}{4\pi}\int_{-\infty}^{\infty}\gamma[\mathrm{e}^{-\gamma h}\bar{f}_1(s)+\bar{f}_2(s)]\,\mathrm{e}^{-\mathrm{i}sx}\,\mathrm{d}s=\tau_0(x),\quad |x|\leqslant l \tag{44}$$

and

$$\bar{f}_{\phi1}(s)=0,\quad \bar{f}_{\phi2}(s)=0,\quad f_{\phi1}(x)=0,\quad f_{\phi2}(x)=0\qquad \text{for all } s \text{ and } x \tag{45}$$

$$\bar{f}_{\psi1}(s)=0,\quad \bar{f}_{\psi2}(s)=0,\quad f_{\psi1}(x)=0,\quad f_{\psi2}(x)=0\qquad \text{for all } s \text{ and } x \tag{46}$$

From Eqs. (41)–(44), it can be obtained

$$\bar{f}_1(s)=\bar{f}_2(s)\Rightarrow f_1(x)=f_2(x),\qquad \tau_{yz}^{(1)}(x,h)=\tau_{yz}^{(2)}(x,h)=\tau_{yz}^{(2)}(x,0)=\tau_{yz}^{(3)}(x,0) \tag{47}$$

$$D_y^{(1)}(x,h)=D_y^{(2)}(x,h)=D_y^{(2)}(x,0)=D_y^{(3)}(x,0) \tag{48}$$

$$B_y^{(1)}(x,h) = B_y^{(2)}(x,h) = B_y^{(2)}(x,0) = B_y^{(3)}(x,0) \tag{49}$$

To determine the unknown functions $\bar{f}_1(s)$ and $\bar{f}_2(s)$, the above two pairs of dual integral equations (41)–(44) must be solved.

4. Solution of the dual integral equations

The Schmidt method (Morse and Feshbach, 1958; Zhou et al., 1999; Zhou and Wang, 2002) is used to solve the dual integral equations. The jumps of the displacements across the crack surfaces are represented by the following series:

$$f_1(x) = f_2(x) = \sum_{n=0}^{\infty} b_n P_n^{\left(\frac{1}{2},\frac{1}{2}\right)}\left(\frac{x}{l}\right)\left(1-\frac{x^2}{l^2}\right)^{\frac{1}{2}} \quad \text{for } -l \leqslant x \leqslant l \tag{50}$$

$$f_1(x) = f_1(x) = w^{(1)}(x,h^+) - w^{(2)}(x,h^-) = w^{(2)}(x,0^+) - w^{(3)}(x,0^-) = 0 \quad \text{for } |x| > l \tag{51}$$

where b_n are unknown coefficients to be determined and $P_n^{(1/2,1/2)}(x)$ is a Jacobi polynomial (Gradshteyn and Ryzhik, 1980). The Fourier transform of Eqs. (50) and (51) is (Erdelyi, 1954)

$$\bar{f}_1(s) = \bar{f}_2(s) = \sum_{n=0}^{\infty} b_n G_n \frac{1}{s} J_{n+1}(sl), \quad G_n = 2\sqrt{\pi}(-1)^n \mathrm{i}^n \frac{\Gamma\left(n+1+\frac{1}{2}\right)}{n!} \tag{52}$$

where $\Gamma(x)$ and $J_n(x)$ are the Gamma and Bessel functions, respectively.

Substituting Eq. (52) into Eqs. (41)–(44), respectively. It can be shown that Eqs. (41) and (42) are automatically satisfied. After integration with respect to x in $[-l,x]$, Eqs. (43) and (44) reduces to

$$\frac{c_{440}}{4\pi}\sum_{n=0}^{\infty} b_n G_n \int_{-\infty}^{\infty} \frac{\mathrm{i}\gamma}{s^2}[1+\mathrm{e}^{-\gamma h}]J_{n+1}(sl)[\mathrm{e}^{-\mathrm{i}sx} - \mathrm{e}^{\mathrm{i}sl}]\,\mathrm{d}s = \int_{-l}^{x} \tau_0(s)\,\mathrm{e}^{-\beta s}\,\mathrm{d}s \tag{53}$$

From the relationships (Gradshteyn and Ryzhik, 1980)

$$\int_0^{\infty} \frac{1}{s} J_n(sa)\sin(bs)\,\mathrm{d}s = \begin{cases} \dfrac{\sin[n\sin^{-1}(b/a)]}{n}, & a \geqslant b \\ \dfrac{a^n \sin(n\pi/2)}{n[b+\sqrt{b^2-a^2}]^n}, & b \geqslant a \end{cases} \tag{54}$$

$$\int_0^{\infty} \frac{1}{s} J_n(sa)\cos(bs)\,\mathrm{d}s = \begin{cases} \dfrac{\cos[n\sin^{-1}(b/a)]}{n}, & a \geqslant b \\ \dfrac{a^n \cos(n\pi/2)}{n[b+\sqrt{b^2-a^2}]^n}, & b \geqslant a \end{cases} \tag{55}$$

the semi-infinite integral in Eq. (53) can be modified as:

$$\begin{aligned}
&\int_{-\infty}^{\infty} \frac{\gamma}{s^2}[1+\mathrm{e}^{-\gamma h}]J_{n+1}(sl)[\mathrm{e}^{-\mathrm{i}sx}-\mathrm{e}^{\mathrm{i}sl}]\,\mathrm{d}s \\
&\quad = \begin{cases} \dfrac{2}{n+1}\left\{\cos\left[(n+1)\sin^{-1}\left(\dfrac{x}{l}\right)\right]-(-1)^{\frac{n+1}{2}}\right\}, & n=1,3,5,7,\ldots \\ \dfrac{-2\mathrm{i}}{n+1}\left\{\sin\left[(n+1)\sin^{-1}\left(\dfrac{x}{l}\right)\right]+(-1)^{\frac{n}{2}}\right\}, & n=0,2,4,6,\ldots \end{cases} \\
&\qquad + \int_0^{\infty} \frac{1}{s}\left[\frac{\gamma-s}{s}+\frac{\gamma}{s}\mathrm{e}^{-\gamma h}\right]J_{n+1}(sl)[\mathrm{e}^{-\mathrm{i}sx}-\mathrm{e}^{\mathrm{i}sl}]\,\mathrm{d}s \\
&\qquad + \int_{-\infty}^{0} \frac{1}{s}\left[\frac{\gamma+s}{s}+\frac{\gamma}{s}\mathrm{e}^{-\gamma h}\right]J_{n+1}(sl)[\mathrm{e}^{-\mathrm{i}sx}-\mathrm{e}^{\mathrm{i}sl}]\,\mathrm{d}s
\end{aligned} \tag{56}$$

Thus the semi-infinite integral in Eq. (53) can be evaluated directly. Eq. (53) can now be solved for the coefficients b_n by the Schmidt method (Morse and Feshbach, 1958; Zhou et al., 1999; Zhou and Wang, 2002). For brevity, Eq. (53) can be rewritten as

$$\sum_{n=0}^{\infty} b_n E_n(x) = U(x), \quad -l \leqslant x \leqslant l \tag{57}$$

where $E_n(x)$ and $U(x)$ are known functions and the coefficients b_n are to be determined. A set of functions $P_n(x)$ which satisfy the orthogonality condition

$$\int_{-l}^{l} P_m(x)P_n(x)\,\mathrm{d}x = N_n\delta_{mn}, \quad N_n = \int_{-l}^{l} P_n^2(x)\,\mathrm{d}x \tag{58}$$

can be constructed from the function, $E_n(x)$, such that

$$P_n(x) = \sum_{i=0}^{n} \frac{M_{in}}{M_{nn}} E_i(x) \tag{59}$$

where M_{ij} is the cofactor of the element d_{ij} of D_n, which is defined as

$$D_n = \begin{bmatrix} d_{00}, d_{01}, d_{02}, \ldots, d_{0n} \\ d_{10}, d_{11}, d_{12}, \ldots, d_{1n} \\ d_{20}, d_{21}, d_{22}, \ldots, d_{2n} \\ \vdots \\ d_{n0}, d_{n1}, d_{n2}, \ldots, d_{nn} \end{bmatrix}, \quad d_{ij} = \int_{-l}^{l} E_i(x)E_j(x)\,\mathrm{d}x \tag{60}$$

Using Eqs. (57)–(60), we obtain

$$b_n = \sum_{j=n}^{\infty} q_j \frac{M_{nj}}{M_{jj}} \quad \text{with } q_j = \frac{1}{N_j}\int_{-l}^{l} U(x)P_j(x)\,\mathrm{d}x \tag{61}$$

5. Intensity factors

The coefficients b_n are known, so that the entire perturbation stress field, the perturbation electric displacement field and the magnetic flux can be obtained. However, in fracture mechanics, it is of importance to determine the perturbation stress τ_{yz}, the perturbation electric displacement D_y and the perturbation

magnetic flux B_y in the vicinity of the crack tips. In the case of the present study, $\tau_{yz}^{(1)}$, $\tau_{yz}^{(2)}$, $\tau_{yz}^{(3)}$, $D_y^{(1)}$, $D_y^{(2)}$, $D_y^{(3)}$, $B_y^{(1)}$, $B_y^{(2)}$ and $B_y^{(3)}$ along the crack line can be expressed respectively as

$$\begin{aligned}\tau_{yz}^{(1)}(x,h) &= \tau_{yz}^{(2)}(x,h) = \tau_{yz}^{(2)}(x,0) = \tau_{yz}^{(3)}(x,0) = \tau_{yz}\\ &= -\frac{c_{440}\,\mathrm{e}^{\beta x}}{4\pi}\sum_{n=0}^{\infty} b_n G_n \int_{-\infty}^{\infty} \frac{\gamma}{s}[1+\mathrm{e}^{-\gamma h}]J_{n+1}(sl)\,\mathrm{e}^{-\mathrm{i}sx}\,\mathrm{d}s\\ &= -\frac{c_{440}\,\mathrm{e}^{\beta x}}{4\pi}\sum_{n=0}^{\infty} b_n G_n \left\{ \int_0^{\infty} J_{n+1}(sl)\,\mathrm{e}^{-\mathrm{i}sx}\,\mathrm{d}s + \int_0^{\infty}\left[\frac{\gamma-s}{s}+\frac{\gamma}{s}\mathrm{e}^{-\gamma h}\right]J_{n+1}(sl)\,\mathrm{e}^{-\mathrm{i}sx}\,\mathrm{d}s \right.\\ &\quad \left. - \int_{-\infty}^{0} J_{n+1}(sl)\,\mathrm{e}^{-\mathrm{i}sx}\,\mathrm{d}s + \int_{-\infty}^{0}\left[\frac{\gamma+s}{s}+\frac{\gamma}{s}\mathrm{e}^{-\gamma h}\right]J_{n+1}(sl)\,\mathrm{e}^{-\mathrm{i}sx}\,\mathrm{d}s \right\} \end{aligned} \tag{62}$$

$$\begin{aligned}D_y^{(1)}(x,h) &= D_y^{(2)}(x,h) = D_y^{(2)}(x,0) = D_y^{(3)}(x,0) = D_y\\ &= -\frac{e_{150}\,\mathrm{e}^{\beta x}}{4\pi}\sum_{n=0}^{\infty} b_n G_n \int_{-\infty}^{\infty} \frac{\gamma}{s}[1+\mathrm{e}^{-\gamma h}]J_{n+1}(sl)\,\mathrm{e}^{-\mathrm{i}sx}\,\mathrm{d}s\\ &= -\frac{e_{15}\,\mathrm{e}^{\beta x}}{4\pi}\sum_{n=0}^{\infty} b_n G_n \left\{ \int_0^{\infty} J_{n+1}(sl)\,\mathrm{e}^{-\mathrm{i}sx}\,\mathrm{d}s + \int_0^{\infty}\left[\frac{\gamma-s}{s}+\frac{\gamma}{s}\mathrm{e}^{-\gamma h}\right]J_{n+1}(sl)\,\mathrm{e}^{-\mathrm{i}sx}\,\mathrm{d}s \right.\\ &\quad \left. - \int_{-\infty}^{0} J_{n+1}(sl)\,\mathrm{e}^{-\mathrm{i}sx}\,\mathrm{d}s + \int_{-\infty}^{0}\left[\frac{\gamma+s}{s}+\frac{\gamma}{s}\mathrm{e}^{-\gamma h}\right]J_{n+1}(sl)\,\mathrm{e}^{-\mathrm{i}sx}\,\mathrm{d}s \right\} \end{aligned} \tag{63}$$

$$\begin{aligned}B_y^{(1)}(x,h) &= B_y^{(2)}(x,h) = B_y^{(2)}(x,0) = B_y^{(3)}(x,0) = B_y\\ &= -\frac{q_{150}\,\mathrm{e}^{\beta x}}{4\pi}\sum_{n=0}^{\infty} b_n G_n \int_{-\infty}^{\infty} \frac{\gamma}{s}[1+\mathrm{e}^{-\gamma h}]J_{n+1}(sl)\,\mathrm{e}^{-\mathrm{i}sx}\,\mathrm{d}s\\ &= -\frac{q_{15}\,\mathrm{e}^{\beta x}}{4\pi}\sum_{n=0}^{\infty} b_n G_n \left\{ \int_0^{\infty} J_{n+1}(sl)\,\mathrm{e}^{-\mathrm{i}sx}\,\mathrm{d}s + \int_0^{\infty}\left[\frac{\gamma-s}{s}+\frac{\gamma}{s}\mathrm{e}^{-\gamma h}\right]J_{n+1}(sl)\,\mathrm{e}^{-\mathrm{i}sx}\,\mathrm{d}s \right.\\ &\quad \left. - \int_{-\infty}^{0} J_{n+1}(sl)\,\mathrm{e}^{-\mathrm{i}sx}\,\mathrm{d}s + \int_{-\infty}^{0}\left[\frac{\gamma+s}{s}+\frac{\gamma}{s}\mathrm{e}^{-\gamma h}\right]J_{n+1}(sl)\,\mathrm{e}^{-\mathrm{i}sx}\,\mathrm{d}s \right\} \end{aligned} \tag{64}$$

An examination of Eqs. (62)–(64), the singular parts of the stress field, the electric displacement field and the magnetic flux can be obtained respectively from the relationship (Gradshteyn and Ryzhik, 1980)

$$\int_0^{\infty} J_n(sa)\cos(bs)\,\mathrm{d}s = \begin{cases} \dfrac{\cos[n\sin^{-1}(b/a)]}{\sqrt{a^2-b^2}}, & a>b \\ -\dfrac{a^n\sin(n\pi/2)}{\sqrt{b^2-a^2}[b+\sqrt{b^2-a^2}]^n}, & b>a \end{cases} \tag{65}$$

$$\int_0^{\infty} J_n(sa)\sin(bs)\,\mathrm{d}s = \begin{cases} \dfrac{\sin[n\sin^{-1}(b/a)]}{\sqrt{a^2-b^2}}, & a>b \\ \dfrac{a^n\cos(n\pi/2)}{\sqrt{b^2-a^2}[b+\sqrt{b^2-a^2}]^n}, & b>a \end{cases} \tag{66}$$

$$\int_{-\infty}^{\infty} J_{n+1}(sl)\,\mathrm{e}^{-\mathrm{i}sx}\,\mathrm{d}s = 0, \quad x>l \tag{67}$$

The singular parts of the stress field, the electric displacement field and the magnetic flux can be expressed respectively as follows for the upper crack ($x > l$):

$$\tau_1 = -\frac{c_{440}\,\mathrm{e}^{\beta x}}{4\pi}\sum_{n=0}^{\infty} b_n G_n\left[\int_0^{\infty} J_{n+1}(sl)\,\mathrm{e}^{-\mathrm{i}sx}\,\mathrm{d}s - \int_{-\infty}^{0} J_{n+1}(sl)\,\mathrm{e}^{-\mathrm{i}sx}\,\mathrm{d}s\right] = \frac{c_{440}\,\mathrm{e}^{\beta x}}{2\pi}\sum_{n=0}^{\infty} b_n G_n Q_n(x) \tag{68}$$

$$D_1 = -\frac{e_{150}\,\mathrm{e}^{\beta x}}{4\pi}\sum_{n=0}^{\infty} b_n G_n\left[\int_0^{\infty} J_{n+1}(sl)\,\mathrm{e}^{-\mathrm{i}sx}\,\mathrm{d}s - \int_{-\infty}^{0} J_{n+1}(sl)\,\mathrm{e}^{-\mathrm{i}sx}\,\mathrm{d}s\right] = \frac{e_{150}\,\mathrm{e}^{\beta x}}{2\pi}\sum_{n=0}^{\infty} b_n G_n Q_n(x) \tag{69}$$

$$B_1 = -\frac{q_{150}\,\mathrm{e}^{\beta x}}{4\pi}\sum_{n=0}^{\infty} b_n G_n\left[\int_0^{\infty} J_{n+1}(sl)\,\mathrm{e}^{-\mathrm{i}sx}\,\mathrm{d}s - \int_{-\infty}^{0} J_{n+1}(sl)\,\mathrm{e}^{-\mathrm{i}sx}\,\mathrm{d}s\right] = \frac{q_{150}\,\mathrm{e}^{\beta x}}{2\pi}\sum_{n=0}^{\infty} b_n G_n Q_n(x) \tag{70}$$

where

$$Q_n(x) = \begin{cases} \dfrac{(-1)^{\frac{n}{2}} l^{n+1}}{\sqrt{x^2-l^2}\left[x+\sqrt{x^2-l^2}\right]^{n+1}}, & n = 0,2,4,6,\ldots \\ \dfrac{\mathrm{i}(-1)^{\frac{n+1}{2}} l^{n+1}}{\sqrt{x^2-l^2}\left[x+\sqrt{x^2-l^2}\right]^{n+1}}, & n = 1,3,5,7,\ldots \end{cases}$$

The singular parts of the stress field, the electric displacement field and the magnetic flux can be expressed respectively as follows for the upper crack ($x < -l$):

$$\tau_2 = -\frac{c_{440}\,\mathrm{e}^{\beta x}}{4\pi}\sum_{n=0}^{\infty} b_n G_n\left[\int_0^{\infty} J_{n+1}(sl)\,\mathrm{e}^{-\mathrm{i}sx}\,\mathrm{d}s - \int_{-\infty}^{0} J_{n+1}(sl)\,\mathrm{e}^{-\mathrm{i}sx}\,\mathrm{d}s\right] = \frac{c_{440}\,\mathrm{e}^{\beta x}}{2\pi}\sum_{n=0}^{\infty} b_n G_n Q_n^*(x) \tag{71}$$

$$D_2 = -\frac{e_{150}\,\mathrm{e}^{\beta x}}{4\pi}\sum_{n=0}^{\infty} b_n G_n\left[\int_0^{\infty} J_{n+1}(sl)\,\mathrm{e}^{-\mathrm{i}sx}\,\mathrm{d}s - \int_{-\infty}^{0} J_{n+1}(sl)\,\mathrm{e}^{-\mathrm{i}sx}\,\mathrm{d}s\right] = \frac{e_{150}\,\mathrm{e}^{\beta x}}{2\pi}\sum_{n=0}^{\infty} b_n G_n Q_n^*(x) \tag{72}$$

$$B_2 = -\frac{q_{150}\,\mathrm{e}^{\beta x}}{4\pi}\sum_{n=0}^{\infty} b_n G_n\left[\int_0^{\infty} J_{n+1}(sl)\,\mathrm{e}^{-\mathrm{i}sx}\,\mathrm{d}s - \int_{-\infty}^{0} J_{n+1}(sl)\,\mathrm{e}^{-\mathrm{i}sx}\,\mathrm{d}s\right] = \frac{q_{150}\,\mathrm{e}^{\beta x}}{2\pi}\sum_{n=0}^{\infty} b_n G_n Q_n^*(x) \tag{73}$$

where

$$Q_n^*(x) = \begin{cases} \dfrac{(-1)^{\frac{n}{2}} l^{n+1}}{\sqrt{x^2-l^2}\left[|x|+\sqrt{x^2-l^2}\right]^{n+1}}, & n = 0,2,4,6,\ldots \\ \dfrac{-\mathrm{i}(-1)^{\frac{n+1}{2}} l^{n+1}}{\sqrt{x^2-l^2}\left[|x|+\sqrt{x^2-l^2}\right]^{n+1}}, & n = 1,3,5,7,\ldots \end{cases}$$

The results of the stress, the electric displacement and the magnetic flux intensity factors at the right tip of the upper crack can be given as follows, respectively.

$$K(l) = \lim_{x\to l^+}\sqrt{2(x-l)}\cdot\tau_1 = \frac{c_{440}\,\mathrm{e}^{\beta l}}{\sqrt{\pi l}}\sum_{n=0}^{\infty}(-1)^n b_n \frac{\Gamma(n+1+\frac{1}{2})}{n!} \tag{74}$$

$$K^D(l) = \lim_{x\to l^+}\sqrt{2(x-l)}\cdot D_1 = \frac{e_{150}\,\mathrm{e}^{\beta l}}{\sqrt{\pi l}}\sum_{n=0}^{\infty}(-1)^n b_n \frac{\Gamma(n+1+\frac{1}{2})}{n!} \tag{75}$$

$$K^B(l) = \lim_{x\to l^+}\sqrt{2(x-l)}\cdot B_1 = \frac{q_{150}\,\mathrm{e}^{\beta l}}{\sqrt{\pi l}}\sum_{n=0}^{\infty}(-1)^n b_n\frac{\Gamma(n+1+\frac{1}{2})}{n!} \tag{76}$$

The results of the stress, the electric displacement and the magnetic flux intensity factors at the left tip of the upper crack can be given as follows, respectively.

$$K(-l) = \lim_{x\to -l^-}\sqrt{2(|x|-l)}\cdot \tau_2 = \frac{c_{440}\,\mathrm{e}^{-\beta l}}{\sqrt{\pi l}}\sum_{n=0}^{\infty} b_n\frac{\Gamma(n+1+\frac{1}{2})}{n!} \tag{77}$$

$$K^D(-l) = \lim_{x\to -l^-}\sqrt{2(|x|-l)}\cdot D_2 = \frac{e_{150}\,\mathrm{e}^{-\beta l}}{\sqrt{\pi l}}\sum_{n=0}^{\infty} b_n\frac{\Gamma(n+1+\frac{1}{2})}{n!} \tag{78}$$

$$K^B(-l) = \lim_{x\to -l^-}\sqrt{2(|x|-l)}\cdot B_2 = \frac{q_{150}\,\mathrm{e}^{-\beta l}}{\sqrt{\pi l}}\sum_{n=0}^{\infty} b_n\frac{\Gamma(n+1+\frac{1}{2})}{n!} \tag{79}$$

6. Numerical calculations and discussion

As discussed in the works (Zhou et al., 1999; Zhou and Wang, 2002), it can be seen that the Schmidt method is performed satisfactorily if the first 10 terms of infinite series in Eq. (57) are retained. The behavior of the sum of the series keeps steady with the increasing number of terms in Eq. (57). The crack surface loading $-\tau_0(x)$ will simply be assumed to be a polynomial of the form as follows:

$$-\tau_0(x) = -p_0 - p_1\left(\frac{x}{l}\right) - p_2\left(\frac{x}{l}\right)^2 - p_3\left(\frac{x}{l}\right)^3 \tag{80}$$

Since the problem is linear, the results can be superimposed in any suitable manner. The results are obtained by taking only one of the four input parameters p_0, p_1, p_2 and p_3 non-zero at a time. The normalized non-homogeneity constant β is varied between −3.0 and 3.0, which covers most of the practical cases. The results of the present paper are shown in Figs. 2–10. From the results, the following observations are very significant:

(i) From the results, it can be shown that the singular stress, the singular electric displacement and the singular magnetic flux in functionally graded piezoelectric/piezomagnetic materials carry the same forms as

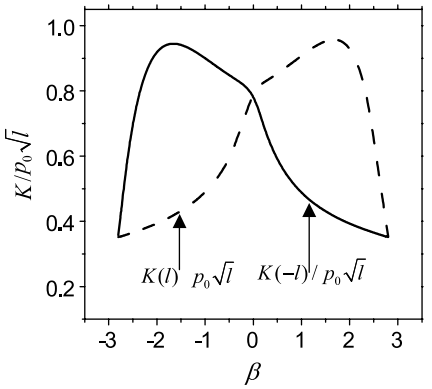

Fig. 2. Influence of βl on the stress intensity factors under the loading $\tau_0(x) = p_0$ for $h/l = 0.5$ and $l = 1.0$.

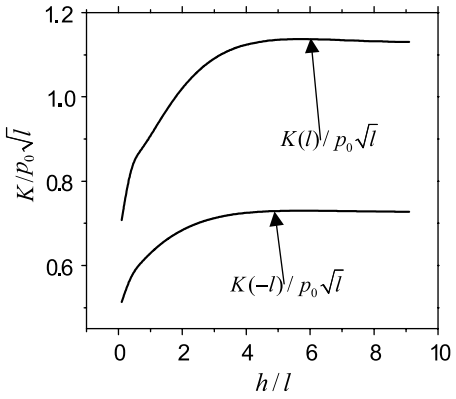

Fig. 3. Influence of h/l on the stress intensity factors under the loading $\tau_0(x) = p_0$ for $\beta = 0.5$ and $l = 1.0$.

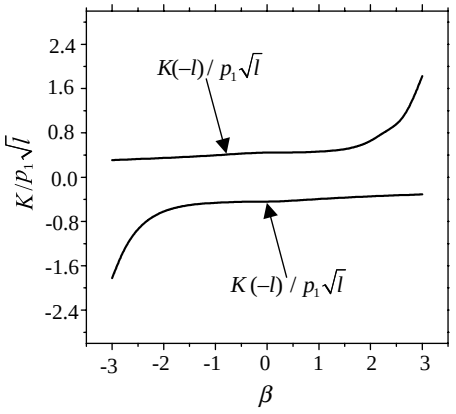

Fig. 4. Influence of β on the stress intensity factors under the loading $\tau_0(x) = p_1(\frac{x}{l})$ for $h/l = 0.5$ and $l = 1.0$.

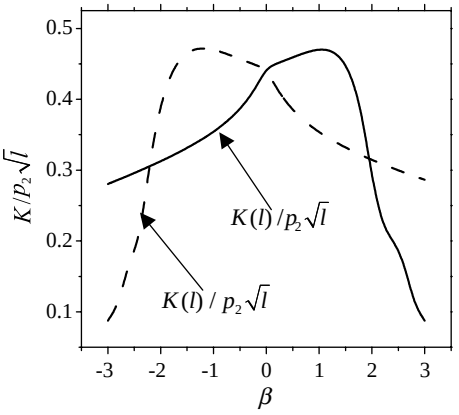

Fig. 5. Influence of β on the stress intensity factors under the loading $\tau_0(x) = p_2(\frac{x}{l})^2$ for $h/l = 0.5$ and $l = 1.0$.

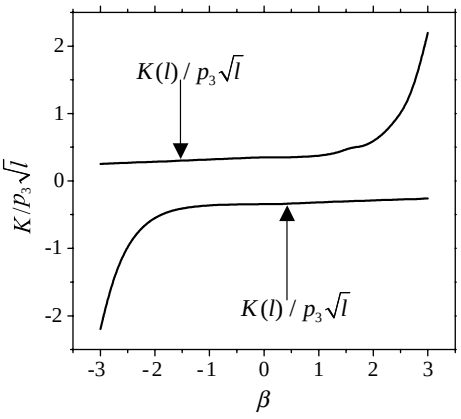

Fig. 6. Influence of β on the stress intensity factors under the loading $\tau_0(x) = p_3(\frac{x}{l})^3$ for $h/l = 0.5$ and $l = 1.0$.

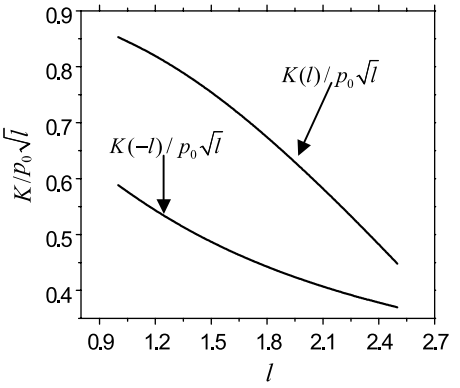

Fig. 7. Influence of l on the stress intensity factors under the loading $\tau_0(x) = p_0$ for $\beta = 0.5$ and $h = 0.5$.

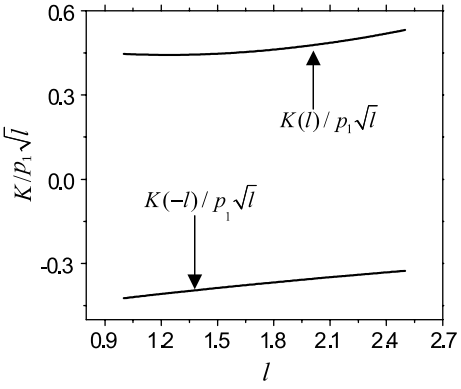

Fig. 8. Influence of l on the stress intensity factors under the loading $\tau_0(x) = p_1(\frac{x}{l})$ for $\beta = 0.5$ and $h = 0.5$.

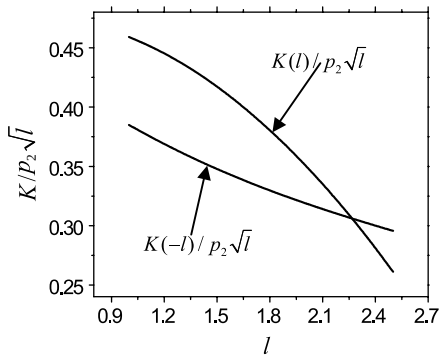

Fig. 9. Influence of l on the stress intensity factors under the loading $\tau_0(x) = p_2(\frac{x}{l})^2$ for $\beta = 0.5$ and $h = 0.5$.

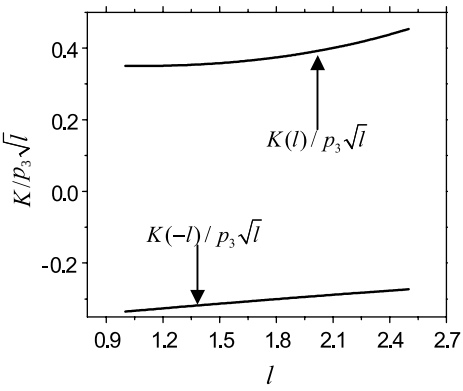

Fig. 10. Influence of l on the stress intensity factors under the loading $\tau_0(x) = p_3(\frac{x}{l})^3$ for $\beta = 0.5$ and $h = 0.5$.

those in a homogeneous piezoelectric/piezomagnetic materials or in a homogeneous piezoelectric materials but the magnitudes of the intensity factors depend significantly upon the gradient of the functionally graded piezoelectric/piezomagnetic materials properties as discussed in the work (Weng and Li, 2002).

(ii) The stress intensity factors do not depend on the material properties. However, the stress intensity factor depends on the non-homogeneity parameter β. This is the same as the anti-plane shear fracture problem in the general non-homogeneity elastic materials. From this we can also obtain that the stress fields are independent of the electric displacement fields and the magnetic fields for the anti-plane shear problem. However, the electric displacement and the magnetic flux intensity factors depend on the non-homogeneity parameter β and the properties of the magneto-electro-elastic composite materials. It can be shown in Eqs. (74)–(79).

(iii) For the symmetric loading, the stress intensity factors at crack tips are symmetric about the line $\beta = 0$ as shown in Figs. 2 and 5. However, for the anti-symmetric loading, the stress intensity factors at crack tips are symmetric about the point $K = 0$ and $\beta = 0$ as shown in Figs. 4 and 6.

(iv) The stress intensity factors increase with the increase in the distance between the parallel cracks as shown in Fig. 3. This phenomenon is called crack shielding effect as discussed in Ratwani's paper (Ratwani and Gupta, 1974). However, the shield effects will be very small for $h/l > 5.0$.

(v) For the symmetric loading as shown in Figs. 2 and 5, the stress intensity factor at the right tip of the crack tends to increase with increase in the functionally graded parameter β, until reaching a maximum at

$\beta = 1.5$, then it decreases in magnitude. However, the stress intensity factor at the left tip of the crack tends to increase with increase in the functionally graded parameter β, until reaching a maximum at $\beta = -1.5$, and then it decreases in magnitude.

(vi) For the anti-symmetric loading as shown in Figs. 4 and 6, the stress intensity factor at the right tip of the crack tends to increase slowly with increase in the functionally graded parameter β until $\beta = 2.0$, and then it increases rapidly in magnitude. However, the stress intensity factor at the left tip of the crack tends to increase rapidly with increase in the functionally graded parameter β until $\beta = -2.0$, and then it increases slowly in magnitude. Hence, the stress intensity factor can be reduced by adjusting the functionally graded parameter β according to the form of the loading.

(vii) The stress intensity factors depend on the crack length. This can be obtained from Eqs. (53) and (62). The dimensionless stress intensity factors do not always increase with the increase in the crack length in functionally graded piezoelectric/piezomagnetic materials under the different anti-plane shear loading as shown in Figs. 7–10. This phenomenon has been discussed in the reference (Shbeeb and Binienda, 1999).

(viii) For the electric displacement and the magnetic flux intensity factors, they have the same changing rule as the stress intensity factor as shown in Eqs. (74)–(79). The results of the electric displacement and the magnetic flux intensity factors can be directly obtained form the results of the stress intensity factors through Eqs. (74)–(79). Here, they are omitted.

Acknowledgements

The authors are grateful for the financial support by the Natural Science Foundation of Hei Long Jiang Province (A0301), the National Natural Science Foundation of China (50232030, 10172030).

References

Avellaneda, M., Harshe, G., 1994. Magnetoelectric effect in piezoelectric/magnetostrictive multiplayer (2-2) composites. Journal of Intelligent Material Systems and Structures 5, 501–513.

Benveniste, Y., 1995. Magnetoelectric effect in fibrous composites with piezoelectric and magnetostrictive phases. Physical Review B 51, 16424–16427.

Chen, J., Liu, Z.X., Zou, Z.Z., 2003. Electromechanical impact of a crack in a functionally graded piezoelectric medium. Theoretical and Applied Fracture Mechanics 39, 47–60.

Delale, F., Erdogan, F., 1988. On the mechanical modeling of the interfacial region in bonded half-planes. ASME Journal of Applied Mechanics 55, 317–324.

Erdelyi, A. (Ed.), 1954. Tables of Integral Transforms, vol. 1. McGraw-Hill, New York.

Fildis, H., Yahsi, O.S., 1996. The axisymmetric crack problem in a non-homogeneous interfacial region between homogeneous half-spaces. International Journal of Fracture 78, 139–163.

Gradshteyn, I.S., Ryzhik, I.M., 1980. Table of Integral, Series and Products. Academic Press, New York.

Harshe, G., Dougherty, J.P., Newnham, R.E., 1993. Theoretical modeling of 3-0/0-3 magnetoelectric composites. International Journal of Applied Electromagnetics in Materials 4, 161–171.

Huang, J.H., Kuo, W.S., 1997. The analysis of piezoelectric/piezomagnetic composite materials containing ellipsoidal inclusions. Journal of Applied Physics 81 (3), 1378–1386.

Jin, D.R., 2003. Functionally graded PZT/ZnO piezoelectric composites. Journal of Materials Science Letters 22, 971–974.

Jin, B., Zhong, Z., 2002. A moving mode-III crack in functionally graded piezoelectric material: permeable problem. Mechanics Research Communications 29, 217–224.

Li, J.Y., 2000. Magnetoelectroelastic multi-inclusion and inhomogeneity problems and their applications in composite materials. International Journal of Engineering Science 38, 1993–2011.

Li, C.Y., Weng, G.J., 2002. Yoffe-type moving crack in a functionally graded piezoelectric material. Proceedings of Royal Society of London A 458, 381–399.

Morse, P.M., Feshbach, H., 1958. In: Methods of Theoretical Physics, vol. 1. McGraw-Hill, New York.

Nan, C.W., 1994. Magnetoelectric effect in composites of piezoelectric and piezomagnetic phases. Physical Review B 50, 6082–6088.

Ozturk, M., Erdogan, F., 1997. Mode I crack problem in an inhomogeneous orthotropic medium. International Journal of Engineering Science 35, 869–883.

Ratwani, M., Gupta, G.D., 1974. Interaction between parallel cracks in layered composites. International Journal of Solids and Structures 10 (7), 701–708.

Shbeeb, N.I., Binienda, W.K., 1999. Analysis of an interface crack for a functionally graded strip sandwiched between two homogeneous layers of finite thickness. Engineering Fracture Mechanics 64, 693–720.

Sih, G.C., Song, Z.F., 2003. Magnetic and electric poling effects associated with crack growth in $BaTiO_3$–$CoFe_2O_4$ composite. Theoretical and Applied Fracture Mechanics 39, 209–227.

Song, Z.F., Sih, G.C., 2003. Crack initiation behavior in magnetoelectroelastic composite under in-plane deformation. Theoretical and Applied Fracture Mechanics 39, 189–207.

Soon, M.K., 2003. Electrical nonlinear anti-plane shear crack in a functionally graded piezoelectric strip. International Journal of Solids and Structures 40, 5649–5667.

Takagi, K., Li, J.F., Yokoyama, S., Watanabe, R., 2003. Fabrication and evaluation of PZT/Pt piezoelectric composites and functionally graded actuators. Journal of the European Ceramic Society 10, 1577–1583.

Van Suchtelen, J., 1972. Product properties: a new application of composite materials. Phillips Research Reports 27, 28–37.

Wang, B.L., 2003. A mode-III crack in functionally graded piezoelectric materials. Mechanics Research Communications 30, 151–159.

Weng, G.J., Li, C.Y., 2002. Antiplane crack problem in functionally graded piezoelectric materials. Journal of Applied Mechanics 69 (4), 481–488.

Wu, T.L., Huang, J.H., 2000. Closed-form solutions for the magnetoelectric coupling coefficients in fibrous composites with piezoelectric and piezomagnetic phases. International Journal of Solids and Structures 37, 2981–3009.

Zhou, Z.G., Wang, B., 2002. The behavior of two parallel symmetry permeable interface cracks in a piezoelectric layer bonded to two half piezoelectric materials planes. International Journal of Solids and Structures 39 (17), 4485–4500.

Zhou, Z.G., Han, J.C., Du, S.Y., 1999. Investigation of a Griffith crack subject to anti-plane shear by using the non-local theory. International Journal of Solids and Structures 36, 3891–3901.